Hamada et al., http://www.jcb.org/cgi/content/full/jcb.201102018/DC1

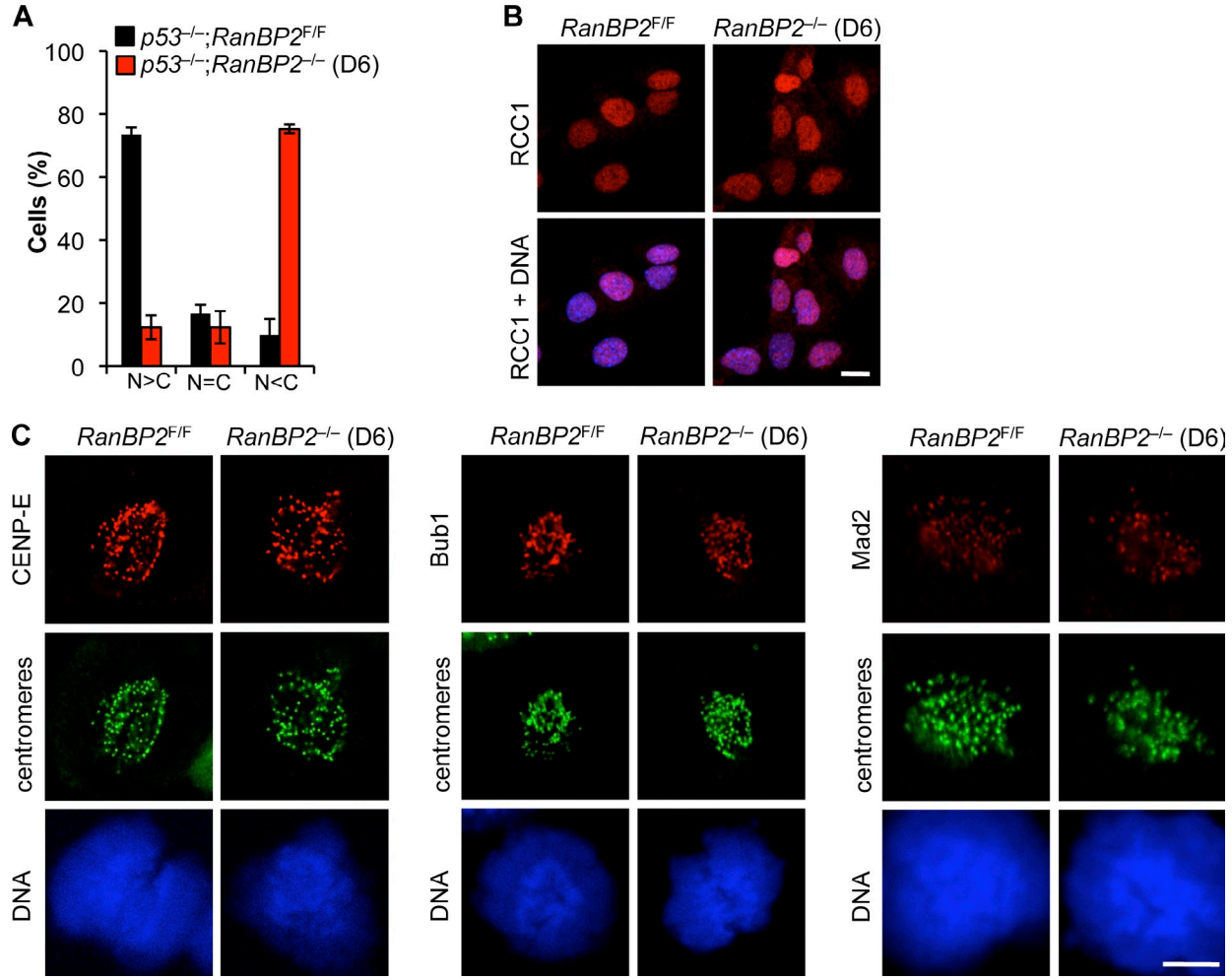

Figure S1. **Subcellular localization of RCC1 and mitotic checkpoint proteins is normal in RanBP2-null MEFs.** (A) *RanBP2*$^{F/F}$ and *RanBP2*$^{-/-}$ (D6) MEFs immortalized by p53 inactivation (*p53*$^{-/-}$) were analyzed for cNLS-mediated protein import using reporter construct Gr_2-GFP_2-cNLS. Importantly, results were similar to those obtained in *RanBP2*$^{F/F}$ and *RanBP2*$^{-/-}$ (D6) MEFs immortalized by SV40 large T antigen expression. These data demonstrate that expression of SV40 large T antigen, which has a cNLS, does not affect the outcome of the nuclear import assay. C, cytoplasm; N, nucleus. (B) Images of RCC1 (red) and DNA (Hoechst; blue) staining of *RanBP2*$^{F/F}$ and *RanBP2*$^{-/-}$ (D6) MEFs at interphase. RCC1 is properly localized to the nucleus in RanBP2-depleted cells. (C) Representative images of *RanBP2*$^{F/F}$ and *RanBP2*$^{-/-}$ (D6) prometaphases stained for the indicated mitotic checkpoint proteins, centromeres, and DNA. Mitotic checkpoint proteins properly target to kinetochores of unattached chromosomes when RanBP2 is lacking. Bars, 10 µm.

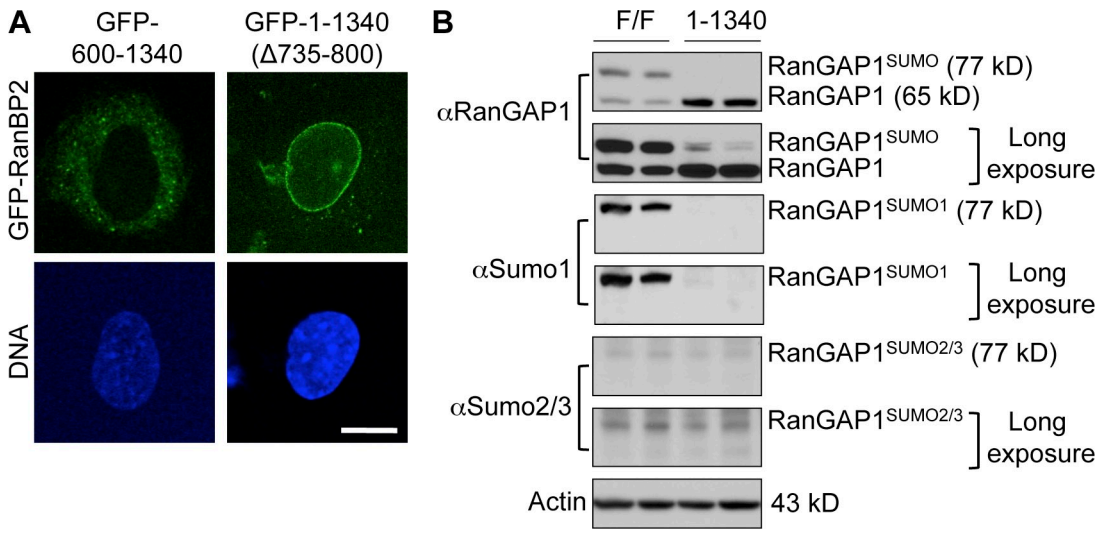

Figure S2. **Little to no SUMO1-modified RanGAP1 accumulates in MEFs lacking the RanBP2 C terminus with the SUMO E3 ligase domain.** (A) Fluorescent images of *RanBP2*$^{-/-}$ (D6) MEFs containing the indicated GFP-tagged RanBP2 mutants. Bar, 10 µm. (B) Western blot analysis of MEF extracts of *RanBP2*$^{F/F}$ and GFP-RanBP2-1–1340 *RanBP2*$^{-/-}$ MEFs probed for the indicated antibodies. Actin served as a loading control. Long and short exposures illustrate that there is little SUMO1-RanGAP1 in the absence of RanBP2 even though overall RanGAP1 levels appear normal. On the other hand, SUMO2/3-RanGAP1 levels seem unaffected in GFP-RanBP2-1–1340 *RanBP2*$^{-/-}$ MEFs.

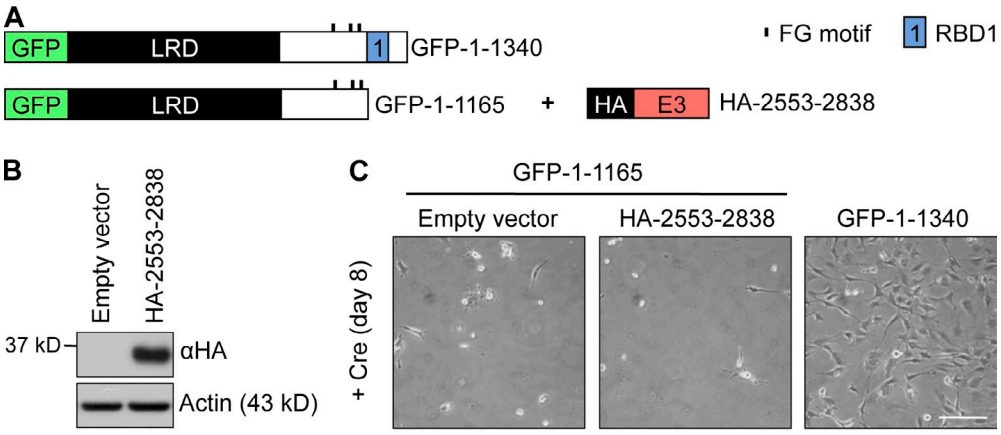

D

Mutant	Growth and survival – Cre	+ Cre
GFP-1-1165 + EV	+	–
GFP-1-1165 + HA-2553-2838	+	–

Figure S3. **RanBP2 SUMO E3 ligase activity cannot rescue cell death of GFP-RanBP2-1–1165 *RanBP2*$^{-/-}$ MEFs.** (A) Schematics of RanBP2 mutants used for survival analysis. (B) Western blot analysis of *RanBP2*$^{F/F}$ cells transduced with empty vector or HA-RanBP2-2553–2838 encoding retrovirus in addition to stable expression of GFP-RanBP2-1–1165. Blots were probed with the indicated antibodies. Actin was used as a loading control. (C) Images of *RanBP2*$^{F/F}$ MEF cultures expressing the indicated RanBP2 mutants captured 8 d after infection with Cre-containing lentivirus. Bar, 200 µm. (D) Viability of *RanBP2*$^{F/F}$ MEFs expressing the indicated RanBP2 proteins in the presence (−Cre) or absence (+Cre) of endogenous RanBP2. EV, empty vector.

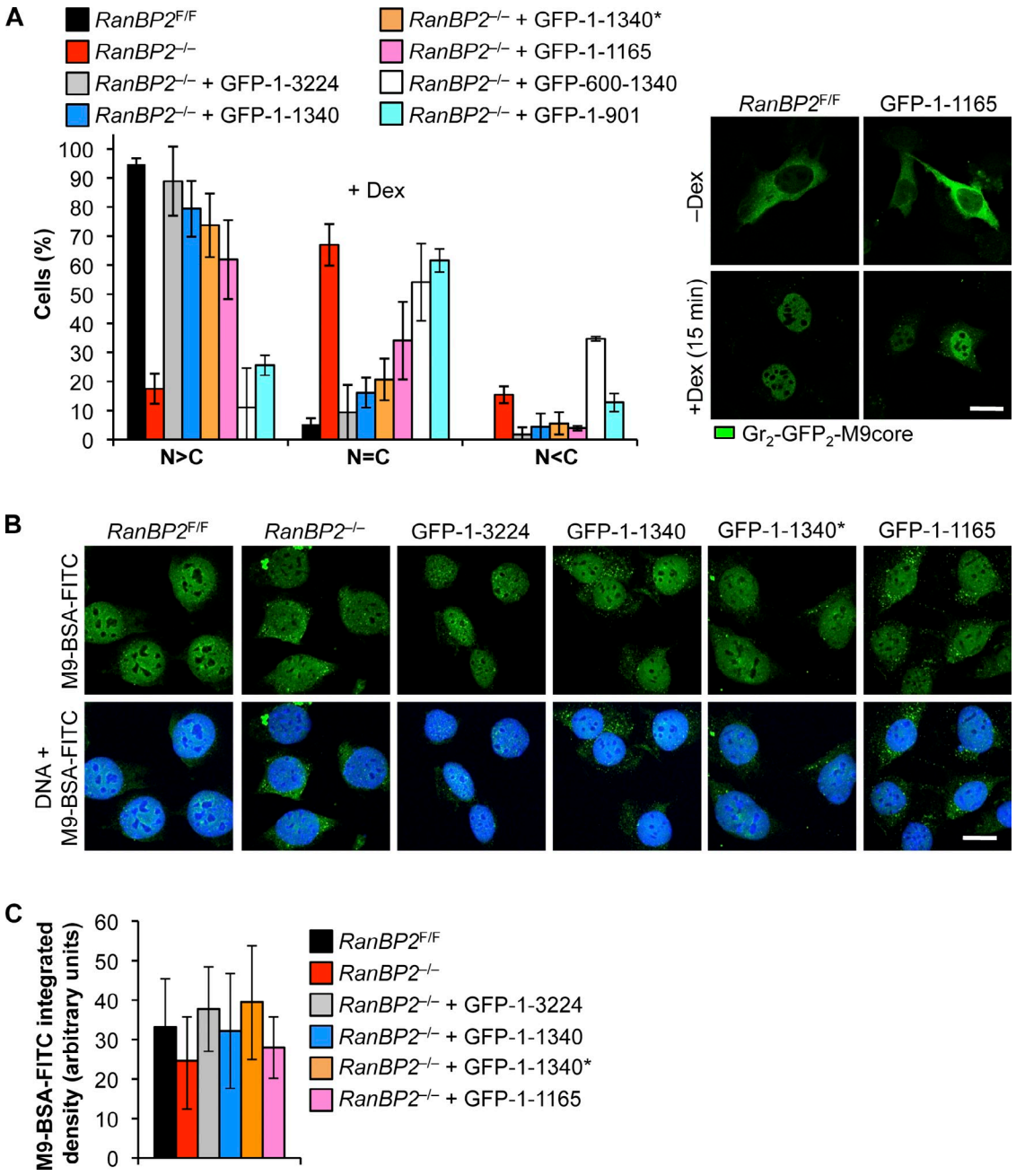

Figure S4. **M9-mediated protein import is not highly dependent on RBD1.** (A) Measurements of Gr_2-GFP_2-M9 protein import in *RanBP2*$^{F/F}$ MEFs and *RanBP2*$^{-/-}$ (D6) MEFs expressing the indicated RanBP2 mutants. Three independent MEF lines were evaluated per genotype (~30 cells per line). Error bars indicate SD. 1–1340*, 1–1340 containing a W1211R and K1212M double mutation in RBD1 designed to disrupt Ran binding and potentiation of RanGAP1; C, cytoplasm; N, nucleus. (B) Transportin-mediated import of M9-BSA-FITC in vitro. Import reactions were performed at RT and stopped after 10 min by fixation. (A and B) Bars, 10 µm. (C) Quantification of nuclear M9-BSA-FITC signals. Error bars indicate SD. All quantifications were performed in three lines, and *n* represents the number of cells/nuclei evaluated (WT, *n* = 75; −Cre, *n* = 90; −/−FL, *n* = 87; −/−1340, *n* = 77; −/−1340*, *n* = 86; −/−1165, *n* = 85).

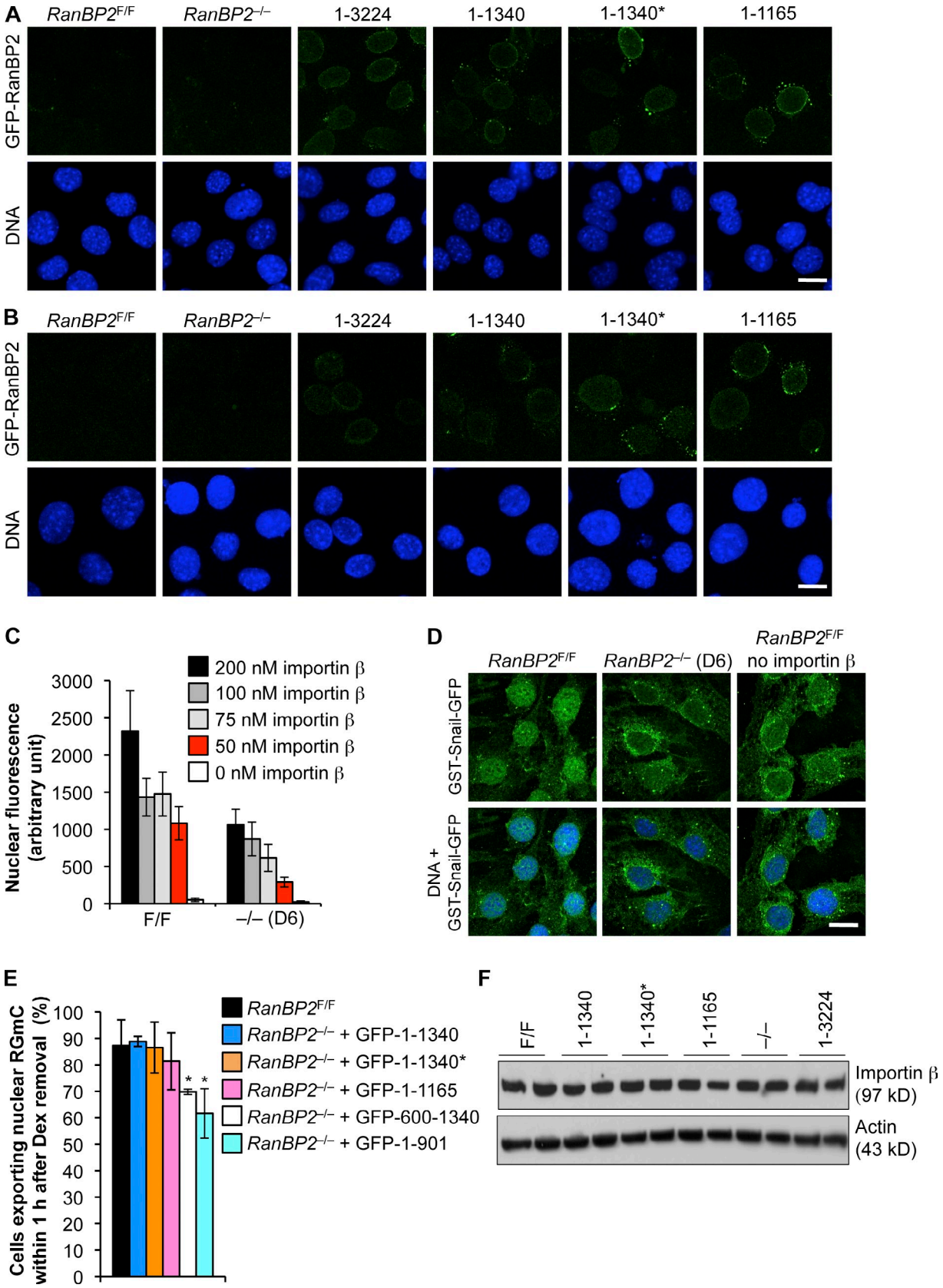

Figure S5. **Transport-related analyses of RanBP2 mutant MEFs.** (A and B) Fluorescence from stably expressed GFP-tagged RanBP2 proteins is very low relative to that of GFP-tagged and FITC-labeled transport cargoes used in our transport assays. Images of *RanBP2*$^{-/-}$ MEFs expressing the indicated GFP-tagged RanBP2 mutants were captured using confocal settings that were identical to those used to visualize transport cargoes in various transport assays. (A) Cells were fixed according to the fixation protocol used in in vivo transport assays (2% PFA for 8 min at RT). Compare signals in A with those in Figs. 7 (B and C) and S4 A. 1–1340*, 1–1340 containing a W1211R and K1212M double mutation in RBD1 designed to disrupt Ran binding and

potentiation of RanGAP1. (B) Cells permeabilized and fixed according to the protocol used in in vitro transport assays (permeabilization with 40 µg/ml digitonin in transport buffer for 8 min on ice and fixed with 3% PFA for 10 min on ice). Compare signals in B with those in Figs. 7 D and S4 B. Bars, 10 µm. (C) An analysis of the effect of importin-β concentration on nuclear import of cNLS-BSA-FITC in *RanBP2*$^{F/F}$ and *RanBP2*$^{-/-}$ (D6) MEFs. In vitro import assays were performed at the indicated importin-β concentrations. Nuclear signals were quantified, and the means of average nuclear fluorescence intensities were plotted (n = 12–16 cells). Error bars represent SD. (D) In vitro import of GST-Snail-GFP by importin-β in *RanBP2*$^{F/F}$ or *RanBP2*$^{-/-}$ (D6) MEFs. Confocal images of cells fixed after a 30-min import reaction at 37°C are shown. Bar, 10 µm. (E) Measurements of RGmC reporter export in *RanBP2*$^{F/F}$ and *RanBP2*$^{-/-}$ (D6) MEFs expressing the indicated RanBP2 mutants. NPC binding and FG repeats are necessary for efficient NES-mediated protein export. *, $P < 0.05$ versus *RanBP2*$^{F/F}$ (two-tailed unpaired t test). Error bars indicate SD. Three independently generated cell lines were used (*RanBP2*$^{-/-}$ + GFP-1–1340, n = 232; *RanBP2*$^{-/-}$ + GFP-1–1340*, n = 244; *RanBP2*$^{-/-}$ + GFP-1–1165, n = 255; *RanBP2*$^{-/-}$ + GFP-600–1340, n = 206; *RanBP2*$^{-/-}$ + GFP-1–901, n = 245). (F) Western blot analysis of MEFs carrying the indicated GFP-tagged RanBP2 expression constructs. Blots were probed with the indicated antibodies.